Optical rogue waves in an all-solid-state laser with a saturable absorber: importance of the spatial effects

2013 J. Opt. 15 064004

(http://iopscience.iop.org/2040-8986/15/6/064004)

IOP PUBLISHING JOURNAL OF OPTICS

J. Opt. **15** (2013) 064004 (6pp) doi:10.1088/2040-8978/15/6/064004

Optical rogue waves in an all-solid-state laser with a saturable absorber: importance of the spatial effects

Carlos Bonazzola[1], **Alejandro Hnilo**[1], **Marcelo Kovalsky**[1] **and Jorge R Tredicce**[2]

[1] Centro de Investigaciones en Láseres y Aplicaciones, CITEDEF-CONICET, Villa Martelli, Argentina
[2] Pole Pluridisciplinaire de la Matière et l' Environnement, Université de la Nouvelle Calédonie, Nouméa—Nouvelle Calédonie, France

E-mail: ahnilo@citedef.gob.ar

Received 21 January 2013, accepted for publication 25 March 2013
Published 4 June 2013
Online at stacks.iop.org/JOpt/15/064004

Abstract
We study the features of the optical rogue waves (ORWs) observed in an all-solid-state (Cr:YAG + Nd:YVO_4) passively-Q-switched laser, which is a system of wide practical interest. The extreme events appear as isolated pulses of extraordinary intensity during the chaotic regime of this laser. The standard theoretical description (three-level rate equations for a single mode of the field and a two-level system for the absorber) does predict the existence of many of the observed dynamical features, including chaos, but it fails to predict the existence of ORWs. Faced with the problem of improving the theoretical description, we find that ORWs are observed only when the Fresnel number of the laser cavity and the embedding dimension of the attractor reconstructed from the experimental time series are high, and the laser spot profile has a spatially complex structure. These results suggest that spatial effects are an essential ingredient in the formation of ORWs in this type of laser.

Keywords: nonlinear laser dynamics, all-solid-state lasers, passive Q-switching

1. Introduction

Rogue waves were originally studied in oceanography, mainly using the nonlinear Schrödinger equation (NLSE). Therefore, it is not surprising to find analogous phenomena in systems that are also ruled by the NLSE, such as the pioneering observations of optical rogue waves (ORW) in micro-structured optical fibers pumped by femtosecond pulses in the threshold of super-continuum spectrum generation [1, 2]. Among the systems ruled by the NLSE in optics, a well-known case is a laser with an intra-cavity absorber having a nonlinear response [3]. In fact, ORWs were observed in one of the chaotic regimes of the Kerr-lens-mode-locked laser [4], which is a system that can be described as a 'laser with a fast saturable absorber'. They were also observed in the passively Q-switched all-solid-state Nd:YAG laser ('laser with a *slow* saturable absorber') [5]. This contribution deals with the observation of ORWs (in the form of self-Q-switching pulses of extraordinary intensity) in the latter of these systems, and the search for the main causes of their formation.

An important issue in the study of ORWs in this laser is that the customary theoretical approach, which is well suited to describe the appearance of even chaotic dynamics, does *not* predict the appearance of ORWs. The results of our theoretical (numerical) study of this problem are presented in section 2. In section 3, we describe the setup: a CW and longitudinally pumped Nd:YVO_4 + Cr:YAG laser. In section 4, we discuss the main experimental results. We find that the oscillation of many spatially transverse modes of the laser cavity is an essential ingredient for the formation of ORWs in this system. This result is in compliance with the ones obtained in related optical systems [6].

Even though the reader is surely familiar with the definition of a rogue wave, it is convenient to state here, for completeness, that the usual quantitative definition of a rogue wave is (i) amplitude higher than twice the average calculated among the set of the 1/3 highest events in the series, which we call the $2AI$ criterion, or (ii) amplitude higher than four (or eight) times the standard deviation, which we call the 4σ (or 8σ) criterion. The limits established by these two definitions can be coincident or not, depending on the form of the probability distribution. For a Gaussian distribution a rogue wave is extremely rare, while, even if remaining an extreme event, it is well known that it may happen more frequently than predicted by Gaussian models. Thus, we expect that rogue waves are described by situations in which the probability distribution presents a long tail (a Levy like distribution). In this paper, we add the value of the *kurtosis* as a quantitative measure of the non-Gaussian feature of a distribution with large wings.

2. Theoretical results

The customary theoretical approach to the system under study is detailed in [7]. It is a simple rate equation model: it devotes one equation to the number of photons in the cavity, three equations to the populations in the lasing levels and the ground state of the active medium, and one to the difference population in the saturable absorber (SA), which is approximated as an ideal two-level system,

$$\begin{aligned}
\mathrm{d}I/\mathrm{d}t &= (2I/t_\mathrm{r})[\sigma_\mathrm{g} l_\mathrm{g}(N_2 - N_1) \\
&\quad - \sigma_\mathrm{a} l_\mathrm{s} N_\mathrm{s} k_\mathrm{A} - k] + \Omega(N_2 - N_1)\gamma_{21} \\
\mathrm{d}N_2/\mathrm{d}t &= PN_0 - (\gamma_{20} + \gamma_{21})N_2 - \sigma_\mathrm{g} cI(N_2 - N_1) \\
\mathrm{d}N_1/\mathrm{d}t &= -\gamma_{10}N_1 + \gamma_{21}N_2 + \sigma_\mathrm{g} cI(N_2 - N_1) \\
\mathrm{d}N_0/\mathrm{d}t &= \gamma_{20}N_2 + \gamma_{10}N_1 - PN_0 \\
\mathrm{d}N_\mathrm{s}/\mathrm{d}t &= \gamma_\mathrm{s}(N_{\mathrm{s}0} - N_\mathrm{s}) - \sigma_\mathrm{a} cIN_\mathrm{s} k_\mathrm{A}
\end{aligned}$$

where I is the photon density inside the laser cavity, the N_i $(i = 0, 1, 2)$ are the population densities in the ground, lower and upper laser transition states, N_s and $N_{\mathrm{s}0}$ are the instantaneous and the initial population densities in the SA. The (usually fixed) parameters σ_g and σ_a are the laser's stimulated emission and the SA's absorber cross sections. l_g and l_s are the lengths of the laser medium and of the SA. c is the speed of light in vacuum and t_r is the cavity round trip time. The γ_{ij} $(i = 1, 2; j = 0, 1)$ are the decay rates of the energy levels, and γ_s is the decay rate of the SA. Ω is the fraction of the spontaneous emission that propagates inside the pumped region; it is determined by the geometry and its exact numerical value has negligible influence on the dynamics after the initial turn-on transient has elapsed (here we take $\Omega = 10^{-4}$). The usual control parameters of this system are the pump rate P, the photon decay rate k and, most important, the ratio k_A between the mode area in the active medium and in the SA, which defines the condition of saturation for Q-switching. In practice, k_A depends of the position of the SA inside the cavity.

In comparison with the NLSE mentioned in the introduction, this model does not make the so-called 'cubic approximation', $E/(1 + |E|^2) \approx E - E|E|^2$, in the saturation of the gain, which is often made to obtain the NLSE from the Maxwell–Bloch equations. This model is therefore able

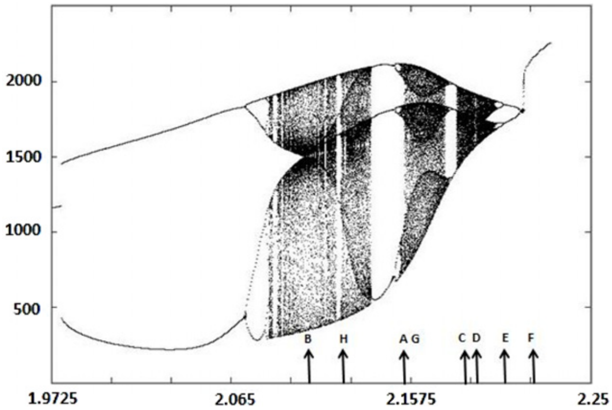

Figure 1. Diagram of bifurcations according to the usual rate equation model in the neighborhood of the laser's operation point. Vertical axis: intensity of the pulses, in arbitrary units. Horizontal axis: ratio k_A of the mode area in the active medium and in the SA. Theoretical time series were analyzed at the k_A values $\{\mathrm{A} \cdots \mathrm{H}\}$ indicated with arrows. Even though chaotic dynamics is found in several cases, no ORWs are found. Pump $P = 668\ \mathrm{s}^{-1}$.

to provide a reliable description even in the case of complete depletion of the population inversion, a situation that can be expected in the presence of high intensity pulses (precisely as ORWs are). It also includes dissipation not present in the NLSE. On the other hand, this model does not include spatially transverse effects. As discussed later, the latter seems to be a crucial limitation in describing the formation of ORWs in this laser.

Numerical runs of this model satisfactorily describe many of the actually observed dynamical features, such as self-Q-switching with pulses of uniform intensity and duration, with a good fitting to the measured values, period doubling (one pulse high, one pulse low), chaotic dynamics, and even a characteristic stable window of period three [7, 8]. Also, the existence of chaos in the pulse spacing variable, showing that there is a deterministic component (not mere noise) in the 'jitter' between pulses, which is a problem of main practical interest [8]. Yet, the model fails to predict the existence of ORWs. This result is curious, because ORWs were easily, immediately and repeatedly observed in a transversely pumped all-solid-state passively Q-switched Nd:YAG laser prototype [5] whose dynamical features were well described by these equations for all other purposes.

We therefore performed a detailed numerical search for ORWs, of which we present here a short summary. In figure 1, we plot the diagram of bifurcations calculated, from numerical runs of the model, in the region near to the working point of the Nd:YAG laser where ORWs were easily observed. The parameter k_A is varied on the horizontal axis. Physically, this means that the SA is displaced inside the laser cavity. All the parameters' values are taken from published tables [9]. Note on the left the first, sudden bifurcation corresponding to the transition from uniform Q-switching (i.e., all the pulses are equal) to period-two at $k_\mathrm{A} = 1.9825$, the bifurcation cascade and the characteristic large stable window of period three. The transition from CW operation to uniform Q-switching occurs at $k_\mathrm{A} = 1.39$ (outside the figure).

In figure 1, the value of k_A increases in steps of 5×10^{-4}, and 500 pulses are plotted for each value of k_A after a transient of 5×10^6 iterations (which is discarded, there is one pulse each $\approx 10^3$ iterations). At the points $\{A \cdots H\}$, where ORWs are thought more likely to appear, the analyzed time series have a length of 10^9 iterations. The points A ($k_A = 2.15$), C ($k_A = 2.1725$), D ($k_A = 2.19$) and E ($k_A = 2.205$) are in the limit between the period-three windows and the chaotic regions, where a behavior with high *sporadicity* (a general concept related with rogue waves) is known to exist for logistic-map-like systems [10]. Looking for ORWs at these points seemed to be a promising strategy, because some of the dynamical features of the rate equations model were shown to be describable (in a rough way) by a map of the same universality class as the logistic map [8]. The points B ($k_A = 2.115$) and F ($k_A = 2.2125$) correspond to the collision of the lower branch of the upper set of bifurcations with the upper branch of the lower set, where ORWs were believed to be likely to appear because of an external crisis. The set of points at G ($k_A = 2.15$) scans the value of the pump rate parameter (from $P = 662$ to $672\ \ \mathrm{s}^{-1}$) at the position $k_A = 2.15$. The point H ($k_A = 2.1375$) is well immersed into the chaotic region. A rich variety of dynamical behavior is found at these points and their neighborhoods, including quasi-periodicity and chaos with a dimension of embedding of the attractor $d_E \leq 4$ and a single positive Lyapunov exponent. The detailed discussion of these interesting theoretical results is long and will be presented elsewhere. What is important to state for our purposes here is that in *no case* are ORWs obtained. The highest intensity value in the series is always well inside the 4σ or the $2IA$ values, and the statistical distribution, even if it is clearly non-Gaussian in some cases, never shows a long tailed L-shape.

The conclusion of this section is the following. Even though the usual rate equation model is able to correctly describe many dynamical issues of the 'all-solid-state laser + slow SA' system, it fails to predict the existence of ORWs. As ORWs were easily observed in practice, the question is what is missing in the model. *Prima facie* candidates are (i) more energy levels in the active medium and/or the SA (solid-state lasers are typical four-level lasers, and a real SA is certainly not a two-level system), (ii) noise enlarging small and otherwise undetectable 'ORW regions' in the space of the parameters, (iii) polarization effects (polarization instabilities in the Nd:YAG laser are often observed), or (iv) the oscillation of more than one transverse mode. Of course, any combination of these four possibilities is also possible. Stated in this way the task is formidable, but the experiments may provide a hint to find out which one among the candidates is the most important. As we will show, there is evidence that the alternative (iv) cannot be excluded, and hence that adding multimode dynamics is the natural first step to enlarge the model to obtain a successful description of ORWs in this system.

3. Experimental setup

We specially built an all-solid-state $Nd{:}YVO_4$ laser. This material produces laser oscillation with a fixed polarization, which allows us to immediately test the candidate (iii) mentioned above.

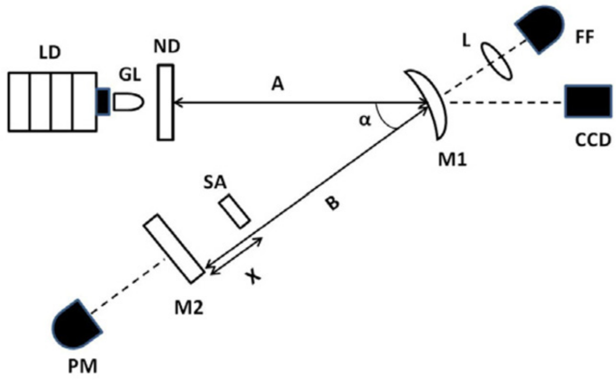

Figure 2. Scheme of the experimental setup. LD: pump laser diode, 2 W CW @808 nm; GL: grin lens; ND: $Nd{:}YVO_4$ slab (active medium); M1: folding mirror ($R = 250$ mm); M2: output mirror (plane); SA: Cr:YAG crystal, transmission (unbleached) 80%; L and FF: focusing lens and fast photodiode; CCD: camera for recording spot images; PM: power meter, $\alpha = 20°$. The position x of the SA is variable, to obtain different dynamical regimes.

The setup is schemed in figure 2. A 2 W (@ 808 nm) CW diode laser is collimated by a grin lens and focused down to a spot 0.12 mm in diameter on a $3 \times 3 \times 1\ \mathrm{mm}^3$ $Nd{:}YVO_4$ crystal, 1% doped and appropriately coated, mounted on a water-cooled copper heatsink. The laser cavity is completed with a folding high reflectivity concave mirror ($R = 250$ mm) and a plane output coupler (reflectivity = 98%). In this way, the mode size varies between the mirrors, with the waist near the output coupler. What we call the *first cavity* has distances between mirrors of $A = 270$ mm and $B = 200$ mm. The CW output power is 300 mW (@ 1064 nm) for 1.8 W pumping. The average output power is measured with the photopile PM placed after the output coupler. One of the loss beams at the folding mirror is focused into a pin fast photodiode (100 ps risetime), connected to a memory digital oscilloscope (350 MHz bandwidth, 5 Gs s^{-1}, memory of 16 MB). This allows recording time series of the self-Q-switching pulse intensities with several thousand pulses and acceptable resolution. In some cases, several oscilloscope runs are added to get longer series. These series are later studied (value of d_E, the Lyapunov exponents, etc) with the TISEAN software package. A CCD camera connected to a PC allows us to observe and record the form of the laser spot. The whole setup is mounted on an optical table with interferometric stability.

A solid-state SA (Cr:YAG crystal, 80% transmission) is placed between the folding mirror and the output coupler at a distance x. The SA is displaced parallel to the cavity axis with the help of a micro-metric translation stage. By adjusting its position, the mode size (at the SA) is varied and hence the condition of saturation and the Q-switching operation are controlled. Typical values of the laser output in the uniform self-Q-switching regime are 200–400 ns FWHM pulses, at a repetition rate of 10–20 kHz and an average output power of 30 mW. As the SA is placed nearer to the output coupler (therefore increasing the value of k_A), we observe that the

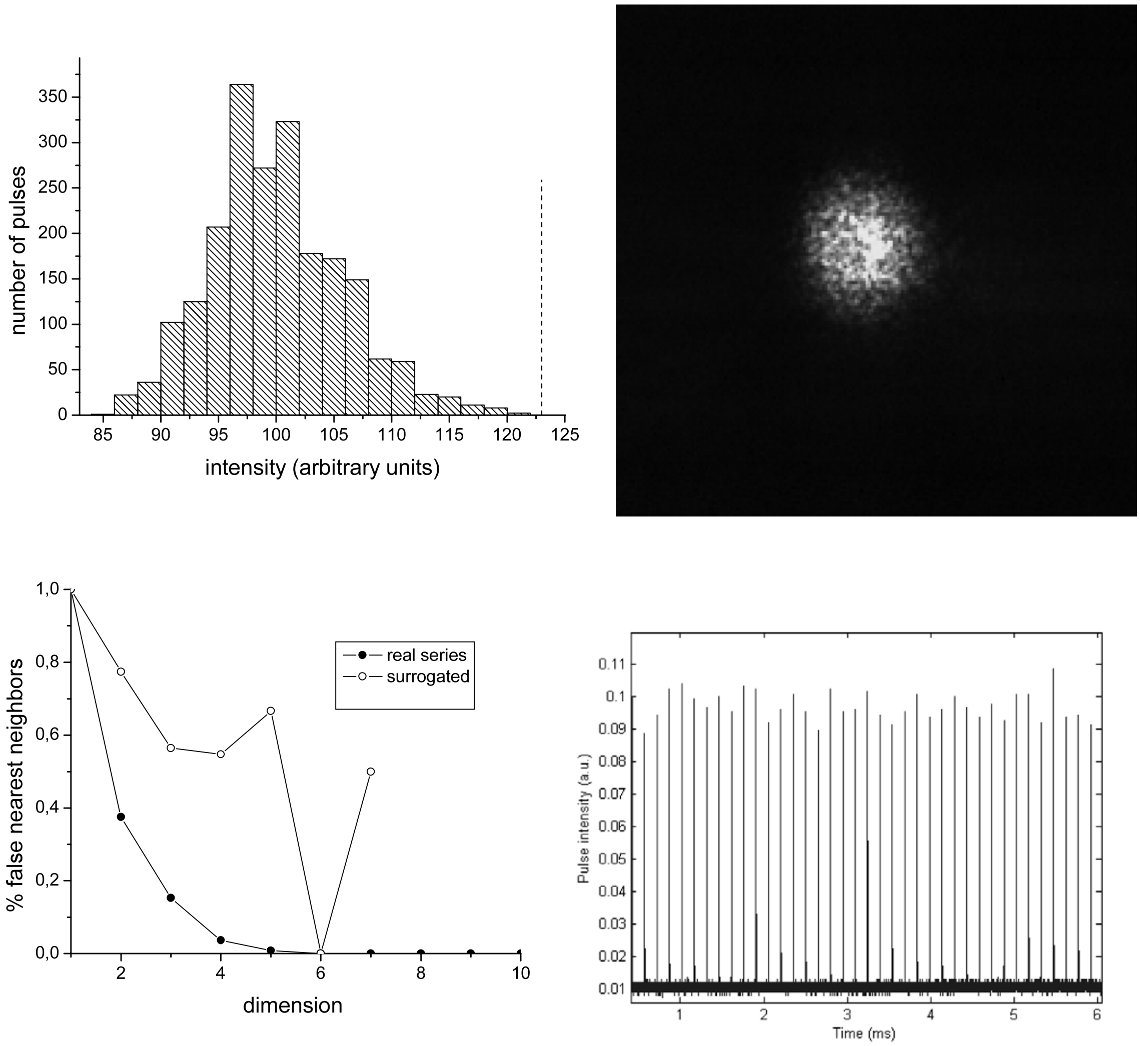

Figure 3. ORWs are not observed, first cavity ($\#F \approx 1$), position of the SA $x = 8$ mm. Upper left: histogram of the pulse intensities. The 4σ threshold for ORWs is 123 (indicated with a vertical dotted line), no pulse surpasses it (maximum intensity: 121), kurtosis = 2, 24. Upper right: image of the laser spot. Lower left: ffn versus d_E for the real and the surrogated series, d_E= 5. Lower right: zoom of the oscilloscope trace. Note that the value of d_E is in reasonable agreement with the theoretical predictions of the rate equation model and the simple structure (TEM_{00}-like) of the spot image.

uniform pulse operation becomes unstable, first showing a two-pulse regime, then a cascade of bifurcations, a chaotic region, a period-three stable window and another chaotic region, in qualitative coincidence with the behavior predicted in figure 1 (the numbers in this figure were calculated for a different cavity, so that no exact agreement could be expected).

We mention here, as a marginal note, that the position of the SA is preferred to the pump as the control parameter because varying the pump modifies the thermal lens in the active medium and hence the cavity design, making the conditions for the observations difficult to determine.

4. Experimental results

An extensive search for ORWs is performed in the chaotic regimes of the *first cavity*. Surprisingly, no ORWs are found. The results corresponding to the recorded time series closest to obtaining ORWs are shown in figure 3. The embedding dimension, measured through the false-nearest-neighbor (ffn) method, is $d_E = 5$, and there is one positive Lyapunov exponent. The highest pulses in the series almost meet the 4σ criterion, but they are far from the other two criteria, and the distribution is not L-shaped. Also the value of the kurtosis is near to the Gaussian value of 3. The intensity of the pulses is rescaled so that their average value is equal to 100. This allows the TISEAN software to work faster and better.

The ORWs so easily observed in the transversely pumped Nd:YAG laser (described in [5]) were not found in the *first cavity*. The apparent difference was the active medium. Was the polarization dynamics essential to the formation of ORWs, after all? After a closer analysis, we found that the value of $(k\gamma_{21})^{1/2}$ (which, as is well known, rules a large part of the dynamics of these lasers) in the Nd:YAG laser was $\approx 10^6\ s^{-1}$, almost three times larger than in the *first cavity*. Therefore,

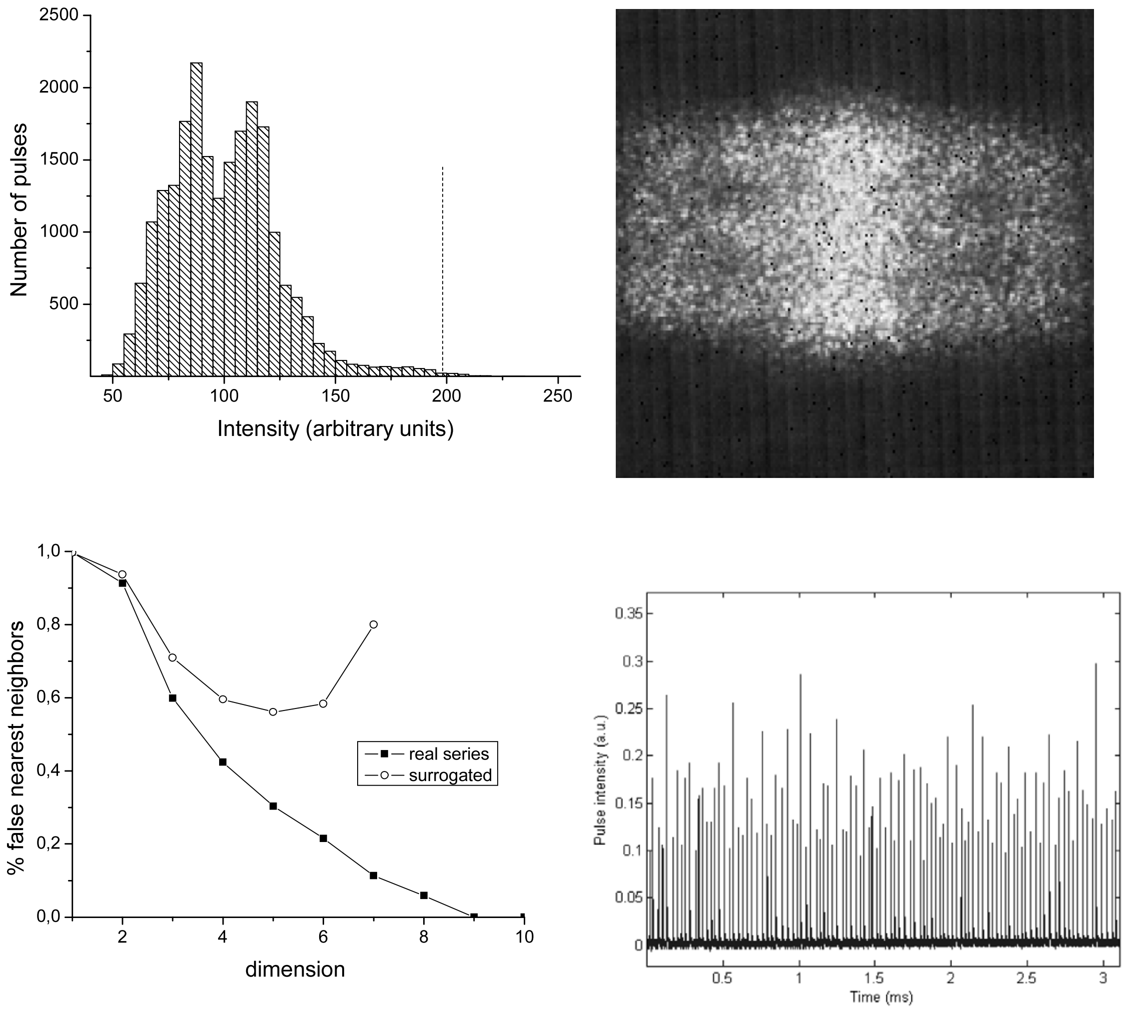

Figure 4. Observation of ORWs, second cavity ($\#F \approx 10$), position of the SA $x = 9$ mm. Upper left: histogram of the pulse intensities, note the L-shape, kurtosis = 4, 65. The 4σ threshold for ORWs is 198 (indicated with a vertical dotted line), there are 60 ORWs (maximum intensity: 252) in a total of 21 918 pulses in the file. Upper right: image of the laser spot. Lower left: ffn versus d_E for the real and the surrogated series. Lower right: zoom of the oscilloscope trace. Note the high value of d_E (=9) and the complex spatial structure of the spot image.

in an effort to return to the situation in [5], we reduced the distance between the mirrors to $A = 120$ mm and $B = 70$ mm (which we call here the *second cavity*) to increase the photon decay rate and put the two values of $(k\gamma_{21})^{1/2}$ as close as possible. ORWs were finally observed but, as discussed below, we do not believe that this change is directly related to the change in the value of $(k\gamma_{21})^{1/2}$. Recall that the numerical simulation was carried out for this parameter value and no ORWs were predicted.

The results corresponding to a time series showing ORWs are displayed, as an illustration, in figure 4. Note the characteristic L-shape and the high kurtosis (=4, 65) of the number of pulses versus intensity distribution. The $d_E = 9$ and the dynamics is chaotic, with two positive Lyapunov exponents. Most interesting, the spot image shows a complex structure with nearly 15 lobes of different intensities. As the position of the SA is varied, a link between the presence of ORWs, a large value of d_E and a spatially structured spot is consistently observed. We then estimated the Fresnel number ($\#F$) of the cavities, as the ratio between the pumped area at the Nd:YVO$_4$ crystal (which acts as the limiting transverse aperture in this laser) and the mode area at the same point. While for the *first cavity* $\#F \approx 1$, for the *second cavity* $\#F \approx 10$, and for the transversely pumped Nd:YAG laser in [5] (where ORWs were most easily observed) $\#F \approx 100$. We find then a direct relationship between the number of oscillating transverse modes of the field inside the laser cavity and the appearance of ORWs. This result is in agreement with the conclusions obtained in an optical system designed to produce ORWs under controllable parameters [6].

It must be noted that a high value of $\#F$ is a condition necessary, but not sufficient, to obtain ORWs in this laser. Besides, the value of x must be adjusted close to the output coupler. The probable reason is that the field must be tightly focused in the SA in order to allow the higher order transverse modes to saturate the absorber, cross the laser threshold and take part in the dynamics to produce the ORWs.

5. Conclusions

We present the first observations and results obtained from a systematical study of the phenomenon of ORWs in a passively

Q-switched, all-solid-state laser (laser with a 'slow' SA). This is a complex phenomenon, so we cannot provide a complete understanding of all of its features at this point. We have found numerical evidence that the customary theoretical approach, which correctly describes many of the dynamical features of this laser, is nevertheless insufficient to predict ORWs. We have also found experimental evidence that transverse spatial effects (which are absent in the customary theoretical approach) play an essential role in the formation of ORWs.

In dealing with transverse effects, there are two possible approaches [11]. One possibility is to project the Maxwell–Bloch equations on a suitable basis. The other approach is to derive global equations (that are still partial differential equations, such as the NLSE) for slowly varying amplitudes. Which of the two approaches is more suitable depends, in general, on the nature of the transverse effects. In cases where the observed transverse patterns have the general structure of a combination of the empty cavity modes, the dynamics is most probably ruled by cavity mode–mode interactions. It is obvious that in this case modal expansion is the natural way to analyze the system. Instead, the global amplitude equation method appears to be more appropriate in cases where periodic patterns, such as stripes and hexagons, or localized structures without a relation with any mode profile, are observed.

In the case under study here, many of the patterns observed in association with ORWs display some symmetry (such as the one in figure 4), therefore suggesting that modal expansion is the suitable approach. A modal expansion was in fact performed in [12] to explain the observation of coupled spatial and temporal instabilities in a laser setup similar to ours, but with a much larger pump rate. In that approach, the number of Hermite–Gaussian modes in the description was increased as the spatial and temporal features became more complex. The observed (stationary, because of the time resolution of the CCD camera) pattern was used as a guide to determine the number and proportion of each Hermite–Gaussian mode in the expansion, even though the real patterns were not stationary. Several dynamical behaviors, mostly related with period doubling bifurcations, were explained in this way. Yet, no ORWs were reported. On the other hand, we observe ORWs also in some cases where the spatial pattern has no apparent relationship with a superposition of empty cavity modes.

Therefore, we think that it is premature to decide now on one or the other of the possible theoretical approaches. We rather prefer to extract more hints from the experiments before attempting the development of a complex numerical model with many parameters, whose values will necessarily be uncertain at this stage of the research. In this sense, we foresee several additional investigations. (1) Adding a second photodiode to record the variation of the intensity at different points of the laser spot, and to measure how the mutual information between the two time series varies according to the different parameters or conditions of operation (namely, with or without ORWs). (2) Obtaining interferograms of the laser spot, to measure the transverse coherence length and the number of domains of coherence. (3) Observing the spectral profile with a high resolution Fabry–Perot to measure the frequency shifts (including mode merging) produced by the mode–mode interaction. We expect that the additional information obtained in this way will serve as a guide to establish a solid foundation for a theoretical explanation of the phenomenon of ORWs in this type of laser.

Finally, it must be mentioned that the all-solid-state self-*Q*-switching laser is a conceptually simple and practically accessible device, being in consequence a convenient toy-system to study ORWs. Besides, it is a laser of main applied interest, so that any improvement in the knowledge of its dynamics will undoubtedly have a large practical impact.

Acknowledgment

This work received support from the PICS '*Dynamique non-linéaire dans les systèmes optiques, atomiques et biologiques*' (DyNLin) CNRS France (2012), no. 05922.

References

[1] Solli D, Ropers C, Koonath P and Jalali B 2007 Optical rogue waves *Nature* **450** 1054
[2] Finot C, Hammami K, Fatome J, Dudley J and Millot G 2010 Selection of extreme events generated in raman fiber amplifiers through spectral offset filtering *IEEE J. Quantum Electron.* **46** 205
[3] Martínez O, Fork R and Gordon J 1985 Theory of passively mode-locked lasers for the case of a nonlinear complex-propagation coefficient *J. Opt. Soc. Am.* B **2** 753
[4] Kovalsky M, Hnilo A and Tredicce J 2011 Extreme events in the Ti:sapphire laser *Opt. Lett.* **36** 4449
[5] Hnilo A, Kovalsky M and Tredicce J 2011 Extreme value events in self-pulsing lasers *IEEE Xplore Paper* 2163377 doi:10.1109/LDNP.2011.6162070
[6] Arecchi F T, Bortolozzo U, Montina A and Residori S 2011 Granularity and inhomogeneity are the joint generators of optical rogue waves *Phys. Rev. Lett.* **106** 153901
[7] Tang D Y, Ng S P, Qin L J and Meng X L 2003 Deterministic chaos in a diode-pumped Nd:YAG laser passively *Q*-switched by a Cr:YAG crystal *Opt.Lett.* **28** 325
[8] Kovalsky M and Hnilo A 2010 Chaos in the pulse spacing of passive *Q*-switched all-solid-state lasers *Opt. Lett.* **35** 3948
[9] Koechner W 1999 *Solid State Laser Engineering* 5th edn (New York: Springer)
[10] Gaspard P and Wang X J 1988 Sporadicity: between periodic and chaotic dynamical behaviors *Proc. Natl Acad. Sci. USA* **85** 4591
[11] Mandel P 1997 *Theoretical Problems in Cavity Nonlinear Optics* (New York: Cambridge University Press)
[12] Wei M-D, Chen C-H and Tu K-C 2004 Spatial and temporal instabilities in a passively *Q*-switched Nd:YAG laser with a Cr:YAG saturable absorber *Opt. Express* **12** 3972